



Since January 2020 Elsevier has created a COVID-19 resource centre with free information in English and Mandarin on the novel coronavirus COVID-19. The COVID-19 resource centre is hosted on Elsevier Connect, the company's public news and information website.

Elsevier hereby grants permission to make all its COVID-19-related research that is available on the COVID-19 resource centre - including this research content - immediately available in PubMed Central and other publicly funded repositories, such as the WHO COVID database with rights for unrestricted research re-use and analyses in any form or by any means with acknowledgement of the original source. These permissions are granted for free by Elsevier for as long as the COVID-19 resource centre remains active.



Identification, synthesis and evaluation of SARS-CoV and MERS-CoV 3C-like protease inhibitors



Vathan Kumar^a, Kian-Pin Tan^b, Ying-Ming Wang^a, Sheng-Wei Lin^a, Po-Huang Liang^{a,b,*}

^a Institute of Biological Chemistry, Academia Sinica, Taipei 115, Taiwan

^b Institute of Biochemical Sciences, National Taiwan University, Taipei 106, Taiwan

ARTICLE INFO

Article history:

Received 31 March 2016

Revised 10 May 2016

Accepted 11 May 2016

Available online 12 May 2016

Keywords:

MERS-CoV

SARS-CoV

3CL^{pro}

Coronavirus

Pyrazolone

ABSTRACT

Severe acute respiratory syndrome (SARS) led to a life-threatening form of atypical pneumonia in late 2002. Following that, Middle East Respiratory Syndrome (MERS-CoV) has recently emerged, killing about 36% of patients infected globally, mainly in Saudi Arabia and South Korea. Based on a scaffold we reported for inhibiting neuraminidase (NA), we synthesized the analogues and identified compounds with low micromolar inhibitory activity against 3CL^{pro} of SARS-CoV and MERS-CoV. Docking studies show that a carboxylate present at either R¹ or R⁴ destabilizes the oxyanion hole in the 3CL^{pro}. Interestingly, **3f**, **3g** and **3m** could inhibit both NA and 3CL^{pro} and serve as a starting point to develop broad-spectrum antiviral agents.

© 2016 Elsevier Ltd. All rights reserved.

1. Introduction

Severe acute respiratory syndrome (SARS) led to a life-threatening form of atypical pneumonia in late 2002. In March 2003, the causative agent was identified and named as SARS coronavirus (SARS-CoV). SARS-CoV belongs to the genus Coronaviridae, and is an enveloped, positive-stranded virus with ~30,000 nucleotides.¹ Viral genome encodes two polyproteins, pp1a (~490 kDa) and pp1ab (~790 kDa). 3C-like protease (3CL^{pro}), the main protease, and papain-like protease (PL^{pro}) cleave these polyproteins to generate non-structural proteins essential for the viral replication.^{2,3} Due to its vital role in replication, 3CL^{pro} is an attractive drug target. Many inhibitors were discovered from high throughput screening and structure-based rational design.^{4–10}

Although the SARS-CoV infection died down soon, another human CoV associated with the Middle East Respiratory Syndrome (MERS-CoV) has recently emerged, killing about 36% (584 of 1621) of patients infected globally, mainly in Saudi Arabia and South Korea.¹¹ Due to the similar maturation pathway, MERS-CoV 3CL^{pro} is also regarded as a target for developing anti-viral drug. The previously reported SARS-CoV 3CL^{pro} inhibitors cannot potently inhibit MERS-CoV 3CL^{pro} without modifications, due to the subtle structural differences in their active sites.¹² Though tremendous efforts have been made to develop inhibitors, therapeutic

interventions for the continuous outbreaks of these deadly CoVs, are yet to reach the market.^{13,14}

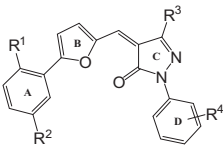
While the origin of SARS dates back to early 2003, influenza has a century-old history of affecting humans. Influenza virus is an enveloped RNA virus that belongs to the orthomyxoviridae family.¹⁵ It has caused four major pandemics in the last century, namely, 1918 ('Spanish' flu, H1N1), 1957 ('Asian' flu, H2N2), 1968 ('Hong Kong' flu, H3N2), and 1977 ('Russian' flu, H1N1).¹⁶ Spanish flu pandemic claimed about 50 million lives worldwide.¹⁷ Recent outbreak of H7N9 in China along with A/Shanghai/1/2013 H7N9 virus with R292K mutation is a serious concern.^{18,19} One of the most accessible targets is neuraminidase (NA), which is essential for the release of viral particle from the cell surface and has been the target for the marketed drugs oseltamivir and zanamivir. We recently reported new inhibitors of both N1 and N2 type NAs and also showed their anti-viral activities in the cell-based assay.²⁰ Due to their structural similarity to our previously discovered SARS-CoV 3CL^{pro} inhibitors,²¹ we screened these NA inhibitors on the SARS-CoV and MERS-CoV 3CL^{pro} and synthesized the analogues of hits to establish the structure–activity–relationship (SAR) on these 3CL^{pro} as reported herein (Table 1).

All the compounds were synthesized as described in Scheme 1. The pyrazolone core was synthesized by the condensation of substituted hydrazines with various β-ketoesters. The substituted aldehydes were synthesized by Meerwein arylation of substituted diazonium salts with furfural.²² Knoevenagel condensation of substituted aldehydes with various pyrazolones in the presence of a

* Corresponding author. Tel.: +886 2 2366 5539; fax: +886 2 2363 5038.

E-mail address: phliang@gate.sinica.edu.tw (P.-H. Liang).

Table 1
IC₅₀ values of analogues against MERS and SARS 3CL^{pro}



Sl. No.	R ¹	R ²	R ³	R ⁴	SARS IC ₅₀ (μM)	MERS IC ₅₀ (μM)
3a	COOH	Cl	CH ₃	3-COOH	>50	>50
3b	COOH	Cl	CF ₃	3-COOH	>50	>50
3c	COOH	H	CF ₃	3-COOH	>50	>50
3d	COOH	Cl	Ph	3-COOH	44.7 ± 5.1	>50
3e	COOH	Cl	CH ₃	H	>50	>50
3f	COOH	Cl	Ph	H	16.4 ± 0.7	12.2 ± 2.2
3g	COOH	Cl	Ph	4-F	20.2 ± 0.3	10.1 ± 1.8
3h	COOH	Cl	Ph	4-CH(CH ₃) ₂	6.0 ± 1.2	7.3 ± 2.1
3i	COOH	Cl	Ph	4-CH(CH ₃) ₃	5.8 ± 1.5	7.4 ± 2.2
3j	H	H	H	H	>50	>50
3k	H	H	Ph	COOH	6.4 ± 1.2	5.8 ± 1.6
3l	H	H	CH ₃	COOH	>50	>50
3m	COOH	H	Ph	H	41.2 ± 9.5	30.3 ± 4.5
3n	COOH	H	Ph	4-F	37.5 ± 0.7	>50
3o	COOH	H	Ph	4-CH(CH ₃) ₂	11.7 ± 2.5	8.9 ± 1.8
3p	COOH	H	Ph	4-CH(CH ₃) ₃	8.6 ± 2.1	7.7 ± 2.2
3q	COOH	H	Ph	4-CN	18.7 ± 4.5	9.6 ± 1.6
3r	COOH	H	Ph	4-OCH ₃	30.7 ± 5.8	8.9 ± 1.8
3s	No ring A		Ph	COOH	>50	>50

catalytic amount of sodium acetate in acetic acid yielded the final compounds (50–88%). Chromatographic purification was not required for most of the compounds as pure compounds could be obtained by methanolic wash.

2. Results and discussion

Absence of NOE signal between the olefinic and R³ phenyl protons in NMR confirmed pyrazolones as a single *E*-isomer.²⁰ However, methyl substitution at R³ gave geometrical isomers (*E/Z*) that was inseparable due to rapid interconversion in solution.²⁰

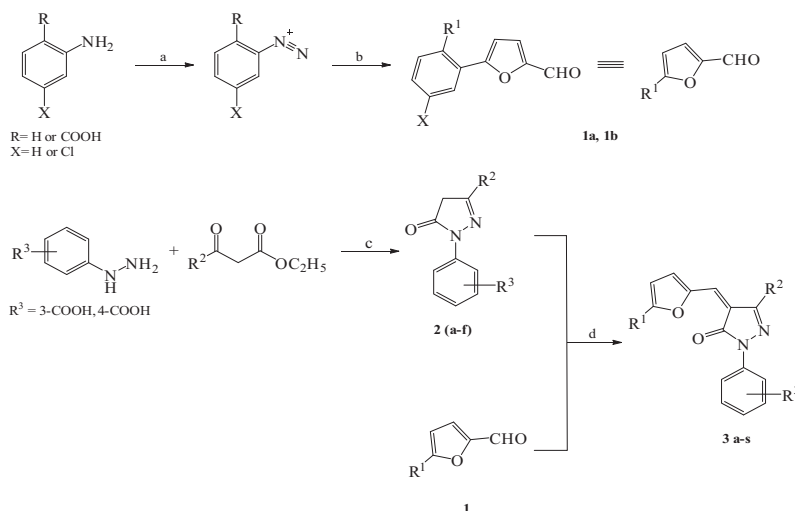
Assay results confirmed that bulkier phenyl group at R³ was essential for the inhibitory activity as compounds **3a–c**, **3e** and **3l** with CH₃ or CF₃ at this position were unable to inhibit SARS 3CL^{pro}. Carboxylate moiety seemed to be an essential component as compound **3j** without it at R¹ and R⁴ was inactive. Removal of R⁴

carboxylate from **3d** (IC₅₀ = 44.7 ± 5.1 μM) but retaining it at R¹ resulted in **3f** (IC₅₀ = 16.4 ± 0.7 μM) with improved activity. Isosteric replacement of hydrogen by fluorine, **3g** (IC₅₀ = 20.2 ± 0.3 μM), caused a slight drop in activity. However, introducing more lipophilic substitution at R⁴ improved activity as seen in case of **3h** (IC₅₀ = 6.0 ± 1.2 μM) and **3i** (IC₅₀ = 5.8 ± 1.5 μM) which had about 3-fold improvement in activity in comparison with **3f**. In contrast, compound **3k** (IC₅₀ = 6.4 ± 1.2 μM) with carboxylate only at R⁴ was 3-fold and 7-fold more potent compared with **3f** and **3m** respectively. From these results we conclude that carboxylate moiety is an important pharmacophore and its presence either at R¹ or R⁴ is critical for the activity as **3k** was as equipotent as **3h** and **3i**. Chlorine at R² slightly changed the activity as we observed 2-fold decrease in the activity of **3m**, **3n**, **3o** and **3p** as compared with **3f**, **3g**, **3h** and **3i** respectively. Substituent on ring D was also important. While compounds with electron-withdrawing F or CN (**3g**, **3q**) did not show significant difference in activity, electron-donating methoxy group (**3r**) on ring D caused 2-fold drop in activity as compared with **3f** without any substituent.

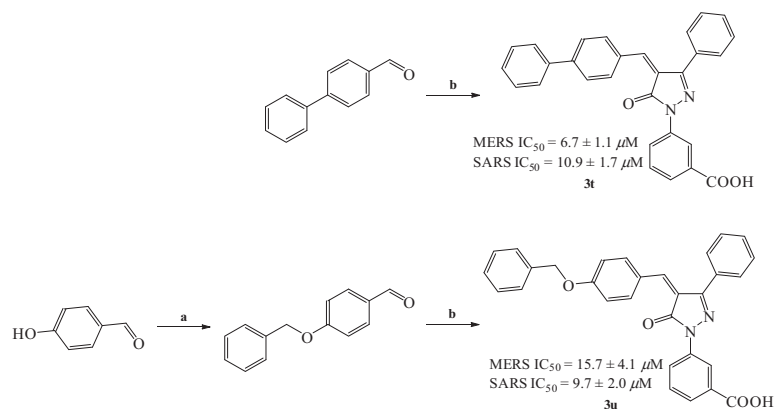
To study the effect of ring B (furan ring), we replaced it with aromatic system to obtain **3t** (Scheme 2). There was no significant change in the activity of **3t** (IC₅₀ = 10.9 ± 1.7 μM) as compared with **3k** (IC₅₀ = 6.4 ± 1.2 μM). Ring A of **3k** was critical as absence of ring A abolished the activity. We then replaced the rigid link between ring A and B with an ether linkage (**3u**) to study the effect. Interestingly, the flexible ether linkage on **3u** (IC₅₀ = 9.7 ± 2.0 μM) (Scheme 2) did not alter activity as compared with **3k** (IC₅₀ = 6.4 ± 1.2 μM).

From this SAR study, we reach a conclusion that pharmacophores phenyl at R³ and carboxylate either at R¹ or R⁴ are essential for the activity. As modification of ring A and B is tolerated well, this can be further altered to enhance the activity of the compounds.

Observed inhibitory activity against SARS 3CL^{pro} was rationalized by docking simulation using ligand bound crystal structure (PDB ID: 2ALV). The docking simulation option (Accurate docking) of iGemdock v2.1 was used to generate 20 solutions. To rationalize the inhibitory effect of these molecules, we must first understand amino acids that constitute the active site of 3CL^{pro}. Active site of 3CL^{pro} can be divided into subsites S1–S6. Subsite S1 is made of vital catalytic residue Cys145 which forms catalytic dyad with His41 to process the polyproteins at eleven sites comprising of conserved Gln followed by small amino acids like Ser, Ala or



Scheme 1. Reagents and conditions: (a) NaNO₂/HCl, 0 °C; (b) furfural, CuCl₂·H₂O, rt, 48 h; (c) AcOH, reflux, 24 h; (d) AcONa–AcOH, reflux, 3 h.



Scheme 2. Reagents and conditions: (a) Benzyl bromide, dry DMF, 0 °C, 3 h; (b) **2f**, AcONa–AcOH, reflux, 3 h.

Gly.²³ Other vital component of S1 subsite is the oxyanion hole, formed by the interaction of C-terminal carboxylate anion of the conserved Gln with Gly143, Ser144 and Cys145, which stabilizes the transition state during proteolysis.^{24,25} Glu166 at the entrance of the pocket interacts via H-bond with Nε2 of the conserved Gln.²⁴ The S2 and S4 subsites contain hydrophobic and bulky side chains like Val, Leu or Phe. Subsites S5 and S6 are near the surface of the active site and has little role in the substrate binding.

Docking (Fig. 1a) shows that compound **3i** with 5.8 μM IC₅₀ binds to SARS 3CL^{PRO} at S1, S1' and S2 subsites to obstruct substrate binding. At S1 subsite, R¹ carboxylate of **3i**, as a representative of **3f–3i** and **3o–3p**, forms H-bonds with Gly143, Ser144 and Cys145 which are the vital residues forming the oxyanion hole. This prevents efficient cleavage of substrate by obstructing stabilization of the tetrahedral intermediate formed during the transition state. The carboxylate moiety of these compounds makes an additional H-bond with His163 at the S1 subsite which is responsible for the specificity of protease towards conserved Gln residue. The furan ring interacts with the hydrophobic side chain of Leu27 in S1' subsite (not shown).

Due to the hydrophobic nature of S2 subsite, additional alkyl substitution on ring D of **3h**, **3i**, **3o** and **3p** enhances interaction with Met49 and Gln189 through hydrophobic contact. This additional contact seems to be responsible for 3-fold enhanced inhibition of **3h** and **3i** compared with **3f** and **3g**. In addition to hydrophobic interaction, carbonyl moiety of pyrazolone core in **3f–3i** and **3o–3p** interacts with His41 through H-bond to destabilize catalytic dyad. Removal of R² chlorine, comparing **3f** and **3g** with **3m** and **3n** respectively, unfavorably reorients the molecule to lose H-bonding with His41, Gly143 and Cys145 (Fig. S1). This explains the observed 2-fold drop in activity on removal of chlorine.

Unlike other compounds in the series, **3k** does not seem to occupy S1' subsite (Fig. 1b). While the carboxylate moiety at R⁴ position interacts with Leu141, Ser144 and His163, R³ phenyl group prefers the hydrophobic pocket S4. Ring A and B being hydrophobic sit well in S2 subsite. Ring A seems to form a weak π–π stacking with His41 and thus destabilizes the catalytic dyad. Nitrogen atom in the pyrazolone core seems to interact with Glu166 located at the entrance of S1 pocket to prevent binding with Gln of the substrate. Modification of **3k** to **3t** and **3u** did not have significant effect as they prefer binding to similar conformation (not shown).

Since 3CL^{PRO} of both MERS-CoV and SARS-CoV are structurally similar, we expressed MERS-CoV 3CL^{PRO} and tested our compounds on it. All SARS-CoV 3CL^{PRO} inhibitors were found to inhibit MERS-CoV 3CL^{PRO} effectively at low micromolar concentrations. Compounds with bulkier groups, electron-withdrawing/donating

or hydrophobic, substituents on ring D had IC₅₀ around 10 μM. Similar to SARS 3CL^{PRO}, presence of carboxylate moiety seemed essential for inhibiting MERS 3CL^{PRO}. Compound **3k** with the carboxylate moiety on ring D was the best inhibitor with IC₅₀ of 5.8 ± 1.6 μM.

For the compounds with carboxylate on ring A and unsubstituted or substituted ring D with less bulkier group like fluorine, removal of chlorine atom caused significant loss of activity by comparing **3f** (12.2 ± 2.2 μM) with **3m** (30.3 ± 4.5 μM) or fluoro-substituted **3g** (10.1 ± 1.8 μM) with **3n** (>50 μM). However, in the presence of bulkier substituents, **3o** (8.9 ± 1.8 μM) and **3p** (7.7 ± 2.2 μM), lost activity of **3m** and **3n** was regained. Removal of chlorine from compounds with bulkier ring D had insignificant effect on inhibition as **3h** (7.3 ± 2.1 μM) and **3i** (7.4 ± 2.2 μM) showed activity similar to **3o** (8.9 ± 1.8 μM) and **3p** (7.7 ± 2.2 μM), respectively.

The recently solved crystal structure (PDB ID: 4YLU) of MERS-CoV 3CL^{PRO} gave insight into the structural difference between the two 3CL^{PRO}.¹² Replacement of residue Thr25 in SARS 3CL^{PRO} with Met25 in case of MERS 3CL^{PRO} has shrunk S2 subsite to prevent latter from accommodating bulkier groups. Unlike SARS-CoV 3CL^{PRO} which accommodates ring A and B of **3k**, smaller S2 subsite of MERS-CoV 3CL^{PRO} accommodates phenyl moiety at R³ (Fig. 2). This smaller size of S2 makes those molecules with the R³ phenyl group fit snugly into the active site of MERS-CoV 3CL^{PRO} and should be the reason behind most of the active compounds being equipotent. In S2 subsite, R³ interacts with His41 via π–π stacking interaction to perturb the catalytic dyad. At S1 subsite our best inhibitor **3k** (Fig. 2), with its carboxylate moiety at ring D, interacts with Ser147 to destabilize oxyanion hole. Carbonyl moiety in pyrazolone core also interacts with Glu169 at the entrance of S2 subsite. At S2 subsite, its R³ phenyl formed π–π stacking with His41 to perturb catalytic dyad. Ring A and B which are primarily hydrophobic interact with the side chains of Leu170, Val193 and Gln195 at S4 subsite. Compound **3f** with unsubstituted phenyl group at R³ prefers hydrophobic S2. The ring C forms T-shaped π–π stacking with His41 and destabilizes the oxyanion hole (Fig. S2a). Removal of chlorine atom caused 3-fold loss in activity of **3m** as compared with **3f** due to loss of T-shaped π–π stacking with His41 (Fig. S2b). In addition, ring D interacts with hydrophobic side chain of Met25. However, when ring D is substituted with bulkier groups, removal of chlorine did not make a significant change in activity as both the molecules maintain similar interactions at S1, S2 and S4 subsites (not shown).

In comparison with inhibiting SARS 3CL^{PRO}, most of the active compounds are more potent on MERS 3CL^{PRO}. In case of **3g**, **3q** and **3r**, the differences in IC₅₀ reach 2 to 3-fold. The smaller size of S2 in MERS 3CL^{PRO} should accommodate the R³ phenyl group

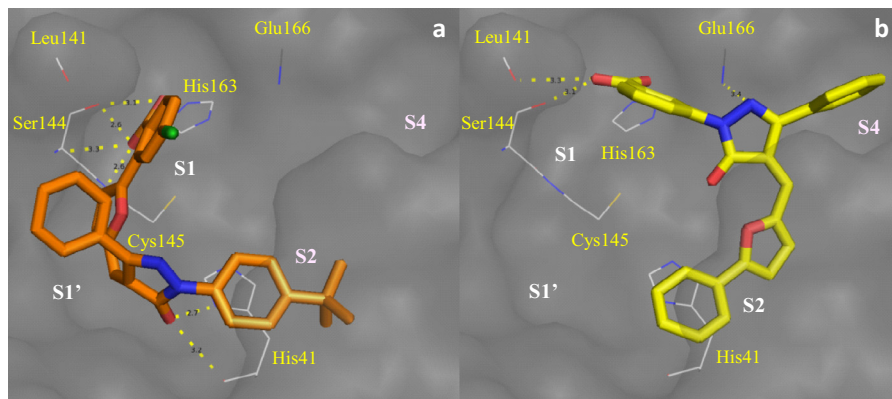


Figure 1. Docking of **3i** (a) with carboxylate at R¹ and **3k** (b) with carboxylate at R⁴ on SARS 3CL^{pro} (PDB ID: 2ALV) in order for carboxylate to form H-bonds with S1 subsite.

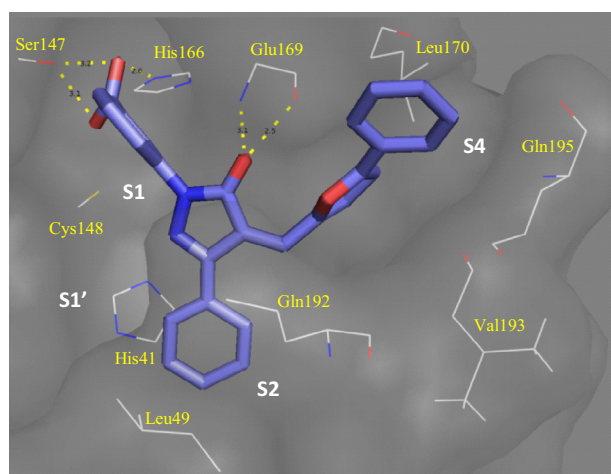


Figure 2. Docking of **3k** on MERS-CoV 3CL^{pro} that has smaller S2 site (PDB ID: 4YLU).

and therefore, the substituted ring D is forced to occupy and make better interaction with the S3 and/or S4 subsites. This point is further illustrated with Figure S3 where the electron density to reflect the shape and size of the active sites and the transparent carbon skeleton of the inhibitor are presented.

It is interesting that compounds **3f**, **3g** and **3m** could inhibit H5N1 neuraminidase (NA) with IC₅₀ of 2.8, 2.9, and 13.7 μM, respectively²⁰ and two 3CL^{pro} at low-micromolar concentrations. Although NA and 3CL^{pro} are not homologous proteins, we observed that they share similar arrangement of the electron-rich amino acid residues in the active sites. While NA contains arginine triad, 3CL^{pro} contains cysteine–histidine dyad in the active site and are essential for substrate processing. These active sites are occupied by mainly two pharmacophores, namely carboxylate and phenyl ring. While carboxylate present at R¹ interacts with the vital arginine residues in case of H5N1 NA,²⁰ it destabilizes the oxyanion hole of MERS 3CL^{pro} (Fig. S4). Another pharmacophore, R³ phenyl interacts with Trp403 and His41 by π–π stacking inside the active site of NA and 3CL^{pro} respectively.

3. Conclusion

Based on a common scaffold, we have optimized the NA inhibitors as inhibitors of 3CL^{pro} of SARS-CoV and MERS-CoV. Thus, we have discovered broad-spectrum inhibitors effective against the drug targets of both coronaviruses and avian influenza virus. To

the best of our knowledge there is no report regarding common inhibitors of these targets from coronavirus and influenza virus in the literature. While there is still no drug for recently emerged MERS-CoV infection, our report raises a possibility of modifying the known inhibitors of NA to inhibit 3CL^{pro} and vice versa. This approach was tried on MERS by using clinically approved drugs.^{26–28} With the escalating cost of drug discovery, concept of drug repurposing is gaining importance. Developing an anti-viral agent with broad-spectrum activity might be advantageous to overcome financial hurdles in the drug discovery. We shall look into modification of the molecules keeping the pharmacophores intact as it seems to be vital for broad-spectrum activity. Compounds with a pyrazole ring surrounded by three hydrophobic groups were also reported to inhibit 3C proteases of human picornaviruses, such as rhinovirus, enterovirus, and coxsackievirus, in addition to 3CL^{pro} of coronaviruses.²⁹ Efforts are being made to co-crystallize these compounds with the enzymes. Cell-based assay would be needed to facilitate further development into more potent inhibitors which could have clinical usefulness.

4. Experimental section

All commercial reagents (Sigma–Aldrich, Acros, Alfa-Aesar) were used as provided and all solvents were of the highest purity. Proton nuclear magnetic resonance (¹H NMR) spectra were recorded on a 400 MHz or 500 MHz spectrometer. Carbon nuclear magnetic resonance (¹³C NMR) spectra were recorded on a 100 MHz or 125 MHz spectrometer. Chemical shifts (δ) are reported in parts per million (ppm) relative to solvent, and the signals are described as br (broad), s (singlet), d (doublet), dd (doublet of doublets), dddd = doublet of doublets of doublets of doublets, t (triplet), and m (multiplet). Coupling constants (*J* values) are given in Hz. High Resolution Mass Spectrometry (HRMS) was obtained by Bruker BioTOF II mass spectrometer and ESI-TOF-MS spectra were recorded. Reaction was monitored on Silica gel 60 F₂₅₄ thin layer plates (TLC) from Merck.

4.1. Preparation of substituted furfural

2-Amino-4-chloro benzoic acid (1.0 equiv) was diazotized with NaNO₂/HCl at 0–5 °C and to this mixture was gradually added furfural (1.2 equiv) in acetone while maintaining temperature around 0–5 °C followed by addition of copper(II) chloride (0.3 equiv) in water at once. The reaction mixture was maintained below 5 °C for 1 h and then allowed to gradually attain room temperature. The reaction was continued at room temperature for 24 h and the precipitate obtained was filtered and washed with methanol–water mixture to obtain pale yellow compound.²⁰

4.1.1. 4-Chloro-2-(5-formylfuran-2-yl)benzoic acid (1a)

¹H NMR (400 MHz, CDCl₃): δ 9.643 (s, 1H), 7.894 (d, *J* = 8.8 Hz, 1H), 7.680 (d, *J* = 2.0 Hz, 1H), dd, *J* = 8.4 Hz, 2.0 Hz, 1H), 7.314 (d, *J* = 4.0 Hz, 1H), 6.821 (d, *J* = 3.6 Hz, 1H). ¹³C NMR (100 MHz, CDCl₃): 178.0 (CH), 168.9 (C), 156.5 (C), 152.8 (C), 136.9 (C), 131.1 (CH), 130.2 (C), 130.1 (C), 129.2 (CH), 128.7 (CH), 123.2 (C), 111.6 (CH). HRMS (*m/z*): [MH⁻] calcd for C₁₂H₁₆ClO₄: 248.9966. Found 248.9967 (4.14 g, 57%).

4.1.2. 2-(5-Formylfuran-2-yl)benzoic acid (1b)

¹H NMR (400 MHz, CDCl₃): δ 9.627 (s, CHO), 7.939 (dd, *J* = 7.5 Hz, 1.2 Hz, 1H), 7.692 (dd, *J* = 7.6 Hz, 1.2 Hz, 1H), 7.617 (td, *J* = 7.6 Hz, 1.6 Hz, 1H), 7.525 (td, *J* = 7.6 Hz, 1.6 Hz, 1H), 7.318 (d, *J* = 3.6 Hz, 1H). ¹³C NMR (100 MHz, CDCl₃): 177.8 (CH), 171.8 (C), 157.9 (C), 152.6 (C), 132.2 (CH), 130.1 (CH), 129.9 (CH), 129.7 (CH), 129.6 (C), 129.4 (C), 122.7 (C), 111.4 (CH). HRMS (*m/z*): [MH⁺] calcd for C₁₂H₉O₄: 217.0501. Found 217.0566 (1.6 g, 20%).

4.2. General procedure for synthesis of pyrazolones

To 1 equiv of β-ketoester in 50 ml of acetic acid was added 1 equiv of substituted phenylhydrazine (for HCl salt 1 equiv of triethylamine was added). The content was refluxed for 24–36 h and the contents cooled and solvent was removed in vacuo. To the precipitate in flask was added ethylacetate to suspend the product and was then filtered to obtain pure compound. Thus obtained product was dried to yield substituted pyrazolone. (Note: In some case product isolated was tautomer due to keto-enol tautomerism.)²⁰

4.2.1. 2,5-Diphenyl-2,4-dihydro-3H-pyrazol-3-one (2a)

¹H NMR (500 MHz, CDCl₃): δ 8.020 (d, *J* = 8.45 Hz, 2H), 7.769 (m, 2H), 7.470 (m, 5H), 7.254 (t, *J* = 7.5 Hz, 1H), 3.760 (s, 2H). ¹³C NMR (125 MHz, CDCl₃): 170.1 (C), 154.5 (C), 138.1 (C), 130.8 (C), 130.6 (CH), 128.8 (CH), 128.7 (CH), 125.9 (CH), 125.1 (CH), 118.9 (CH), 39.43 (CH₂). HRMS (*m/z*): [MH⁻] calcd for C₁₅H₁₁N₂O: 235.0882. Found 235.0880 (6.12 g, 75%).

4.2.2. 3-(3-Methyl-5-oxo-4,5-dihydro-1H-pyrazol-1-yl)benzoic acid (2b)

¹H NMR (400 MHz, MeOD): δ 8.256 (s, 1H), 7.878 (t, *J* = 8.0 Hz, 2H), 7.537 (t, *J* = 8.0 Hz, 2H), 2.200 (s, 3H). ¹³C NMR (100 MHz, MeOD): 169.0 (C), 151.7 (C), 138.8 (C), 133.1 (C), 130.3 (CH), 129.9 (C), 128.1 (CH), 127.0 (C), 126.6 (CH), 124.0 (C), 123.3 (CH), 120.9 (C). HRMS (*m/z*): [MH⁺] calcd for C₁₁H₁₀N₂O₃: 218.0697. Found 218.0764 (0.99 g, 74%).

4.2.3. 2-(4-Methoxyphenyl)-5-phenyl-2,4-dihydro-3H-pyrazol-3-one (2c)

¹H NMR (400 MHz, CDCl₃): δ 7.842–7.811 (m, 2H), 7.744–7.720 (m, 2H), 7.435–7.419 (m, 3H), 6.955–6.915 (m, 2H). ¹³C NMR (100 MHz, CDCl₃): 169.9 (C), 157.1 (C), 154.5 (C), 131.4 (C), 130.9 (C), 130.5 (CH), 128.8 (CH), 125.8 (CH), 120.9 (CH), 114.0 (CH), 55.43 (-OCH₃), 39.38 (CH₂). HRMS (*m/z*): [MH⁺] calcd for C₁₆H₁₅N₂O₂: 267.1134. Found 267.1128.

4.2.4. 4-(5-Oxo-3-phenyl-4,5-dihydro-1H-pyrazol-1-yl)benzotrile (2d)

¹H NMR (400 MHz, CDCl₃): δ 8.193–8.168 (m, 2H), 7.780–7.756 (m, 2H), 7.712–7.697 (m, 2H), 7.493–7.449 (m, 3H). ¹³C NMR (100 MHz, CDCl₃): 170.5 (C), 155.6 (C), 141.5 (C), 133.1 (CH), 131.3 (CH), 130.3 (C), 129.0 (CH), 126.1 (CH), 118.8 (CH), 118.4 (C), 108.0 (C), 39.72 (CH₂). HRMS (*m/z*): [MH⁺] calcd for C₁₆H₁₁N₃O: 262.0980. Found 262.0896.

4.2.5. 3-(5-Oxo-3-phenyl-4,5-dihydro-1H-pyrazol-1-yl)benzoic acid (2f)

¹H NMR (400 MHz, DMSO-*d*₆): δ 13.133 (br, s, COOH), 12.023 (br, s, OH), 8.430 (t, *J* = 2.2 Hz, 1H), 8.108–8.082 (m, 1H), 7.844 (dd, *J* = 9.05 Hz, 1.45 Hz, 1H), 7.621 (t, *J* = 9.9 Hz, 1H), 7.433 (t, *J* = 9.4 Hz, 2H), 7.348 (t, *J* = 9.1 Hz, 1H), 6.040 (s, 1H). ¹³C NMR (100 MHz, DMSO-*d*₆): 167.3 (C), 154.5 (C), 150.5 (C), 139.5 (C), 133.6 (C), 132.1 (C), 129.8 (CH), 129.1 (CH), 128.5 (CH), 126.7 (CH), 125.7 (CH), 125.3 (CH), 121.7 (CH), 85.8 (CH). HRMS (*m/z*): [MH⁺] calcd for C₁₆H₁₃N₂O₃: 281.0926. Found 281.0917 (1.34 g, 49%).

4.3. Preparation of substituted pyrazolone (3a–3s)

Equimolar amount of **1** and **2** were taken in acetic acid and to this was added catalytic amount of sodium acetate (0.1 equiv). As the contents were refluxed the product started to precipitate. The reaction was continued for 3 h and the solvent was removed in vacuo followed by the addition of methanol–water mixture and filtering crude compound which was again thoroughly washed with methanol–water mixture to remove the impurities and any traces of starting material to get final compounds. Some compounds were purified using flash column using ethylacetate: hexane: acetic acid as solvent system.²⁰

4.3.1. 2-(5-((1-(3-Carboxyphenyl)-3-methyl-5-oxo-1,5-dihydro-4H-pyrazol-4-ylidene)methyl)furan-2-yl)-4-chlorobenzoic acid (3a)

¹H NMR (500 MHz, DMSO-*d*₆): δ 13.18 (s, COOH), 8.707 (d, *J* = 4.0 Hz, 1H), 8.574 (t, *J* = 2.0 Hz, 1H), 8.199 (ddd, *J* = 8.1 Hz, 2.5 Hz, 1.0 Hz, 1H), 7.982 (d, *J* = 2.0 Hz, 1H), 7.769–7.752 (m, 2H), 7.688 (s, 1H), 7.646 (d, *J* = 2.5 Hz, 8.0 Hz, 1H), 7.591–7.559 (m, 1H), 7.301 (d, *J* = 4.0 Hz, 1H), 2.531 (s, 3H). ¹³C NMR (125 MHz, DMSO-*d*₆): 168.9 (C), 167.5 (C), 162.2 (C), 157.1 (C), 151.6 (C), 151.0 (C), 138.9 (C), 136.2 (C), 132.3 (C), 132.0 (C), 131.6 (CH), 131.1 (C), 130.4 (C), 130.2 (CH), 130.0 (CH), 129.8 (C), 129.4 (C), 128.7 (CH), 127.1 (CH), 125.5 (CH), 122.3 (CH), 122.1 (C), 119.0 (CH), 115.0 (CH). HRMS (*m/z*): [MH⁻] calcd for C₂₃H₁₄ClN₂O₆: 449.0546. Found 449.0542 (0.216 g, 66%).

4.3.2. 2-(5-((1-(3-Carboxyphenyl)-5-oxo-3-(trifluoromethyl)-1,5-dihydro-4H-pyrazol-4-ylidene)methyl)furan-2-yl)-4-chlorobenzoic acid (3b)

¹H NMR (400 MHz, DMSO-*d*₆): δ 13.38 (s, COOH), 8.871 (d, *J* = 3.2 Hz, 1H), 8.439 (t, *J* = 1.6 Hz, 1H), 8.127 (d, *J* = 8.0 Hz, 1H), 8.079 (d, *J* = 1.2 Hz, 1H), 7.891 (d, *J* = 7.6 Hz, 1H), 7.803 (d, *J* = 8.4 Hz, 1H), 7.718 (m, 3H), 7.437 (d, *J* = 3.2 Hz, 1H). ¹³C NMR (100 MHz, DMSO-*d*₆): 168.8 (C), 167.2 (C), 161.4 (C), 159.7 (C), 150.8 (C), 138.0 (C), 136.3 (C), 132.2 (C), 131.7 (CH), 131.4 (C), 130.6 (CH), 130.0 (CH), 129.1 (CH), 128.9, 127.2 (CH), 123.9 (CH), 120.4 (CH), 116.2 (CH), 115.3 (CH). HRMS(*m/z*): [MH⁺] calcd for C₂₃H₁₃ClF₃N₂O₆: 505.0420. Found 505.0409 (0.119 g, 59%).

4.3.3. 2-(5-((1-(3-Carboxyphenyl)-5-oxo-3-(trifluoromethyl)-1,5-dihydro-4H-pyrazol-4-ylidene)methyl)furan-2-yl)benzoic acid (3c): (e/z mixture)

¹H NMR (500 MHz, DMSO-*d*₆): δ 13.29 (s, 2-COOH), 8.128 (d, *J* = 7.5 Hz, 1H), 7.949 (d, *J* = 7.5 Hz, 1H), 7.880 (d, *J* = 8.0 Hz, 1H), 7.775 (d, *J* = 7.5 Hz, 1H), 7.703–7.606 (m, 4H), 7.359 (d, *J* = 4.0 Hz, 1H). ¹³C NMR (125 MHz, DMSO-*d*₆): 169.6 (C), 167.2 (C), 162.0 (C), 161.5 (C), 150.6 (C), 138.1 (C), 132.8 (C), 132.2 (C), 131.6 (CH), 131.1 (CH), 130.5 (CH), 130.0 (CH), 129.7 (CH), 127.1 (CH), 127.0 (C), 123.9 (CH), 127.1 (C), 127.0 (C), 123.9 (C), 120.4 (CH), 115.4 (CH), 114.5 (C). HRMS (*m/z*): [MH⁻] calcd for C₂₃H₁₃F₃N₂O₆: 469.0647. Found 469.0633 (0.020 g, 4%).

4.3.4. 2-(5-((1-(3-Carboxyphenyl)-5-oxo-3-phenyl-1,5-dihydro-4H-pyrazol-4-ylidene)methyl)furan-2-yl)-4-chlorobenzoic acid (3d)

¹H NMR (500 MHz, DMSO-*d*₆): δ 13.29 (s, COOH), 8.800 (d, *J* = 3.7 Hz, 1H), 8.637 (t, *J* = 1.9 Hz, 1H), 8.264 (ddd, *J* = 8.3 Hz, 2.0 Hz, 0.9 Hz, 1H), 7.998 (d, *J* = 2.1 Hz, 1H), 7.816–7.753 (m, 4H), 7.733 (d, *J* = 8.3 Hz, 1H), 7.627–7.595 (m, 5H), 7.560 (s, 1H), 7.345 (d, *J* = 4.0 Hz, 1H). ¹³C NMR (125 MHz, DMSO-*d*₆): 168.9 (C), 167.4 (C), 162.3 (C), 157.6 (C), 152.3 (C), 151.0 (C), 138.8 (C), 136.1 (C), 132.0 (C), 131.5 (CH), 131.2 (C), 130.7 (C), 130.5 (CH), 130.1 (CH), 129.8 (CH), 129.6 (CH), 129.1 (C), 129.0 (CH), 128.7 (CH), 128.0 (CH), 126.1 (CH), 122.9 (CH), 120.5 (C), 119.5 (CH), 115.3 (CH). HRMS (*m/z*): [MH⁺] calcd for C₂₈H₁₈ClN₂O₆: 513.09. Found 513.0997 (0.145 g, 71%).

4.3.5. 4-Chloro-2-(5-((3-methyl-5-oxo-1-phenyl-1,5-dihydro-4H-pyrazol-4-ylidene)methyl)furan-2-yl)benzoic acid (3e)

¹H NMR (400 MHz, DMSO-*d*₆): 8.690 (d, *J* = 4.0 Hz, 1H), 7.958–7.912 (m, 3H), 7.779 (d, *J* = 8.0 Hz, 1H), 7.645 (m, 2H), 7.460 (m, 2H), 7.278 (d, *J* = 4.0 Hz, 1H), 7.213 (m, 2H), 2.475 (s, 3H –CH₃), 2.321 (s, 3H, –CH₃). ¹³C NMR (100 MHz, DMSO-*d*₆): 168.9, 162.0, 156.9, 151.0, 138.7, 136.2, 132.3, 133.6 (CH), 131.1 (CH), 130.0 (CH), 129.8 (CH), 129.5 (CH), 129.4 (CH), 128.7 (CH), 126.9 (CH), 125.0 (CH), 122.4, 118.6 (CH), 118.3 (CH), 114.9 (CH), 114.6 (CH), 17.73, 13.30 (–CH₃), 13.29 (–CH₃). HRMS (*m/z*): [MH[–]] calcd for C₂₂H₁₄ClN₂O₄: 405.0642. Found 405.0641.

4.3.6. 4-Chloro-2-(5-((5-oxo-1,3-diphenyl-1,5-dihydro-4H-pyrazol-4-ylidene)methyl)furan-2-yl)benzoic acid (3f)

¹H NMR (500 MHz, DMSO-*d*₆): δ 8.983 (d, *J* = 4.0 Hz, 1H), 8.193 (d, *J* = 7.5 Hz, 2H), 7.995 (d, *J* = 1.5 Hz, 1H), 7.922 (d, *J* = 8.5 Hz, 1H), 7.875–7.857 (m, 2H), 7.707 (s, 1H), 7.681–7.643 (m, 4H), 7.550 (t, *J* = 8.5 Hz, 3H), 7.338 (d, *J* = 4.0 Hz, 1H), 7.307 (t, *J* = 7.0 Hz, 1H). ¹³C NMR (125 MHz, DMSO-*d*₆): 169.0 (C), 162.2 (C), 157.5 (C), 152.0 (C), 151.0 (C), 138.6 (C), 136.1 (C), 131.6 (C), 131.5 (CH), 131.2 (CH), 130.8 (C), 130.4 (CH), 130.1 (CH), 129.6 (CH), 129.4 (CH), 129.2 (C), 129.1 (C), 129.0 (CH), 128.7 (CH), 127.7 (C), 125.5 (CH), 120.7 (C), 119.3 (CH), 115.2 (CH). HRMS (*m/z*): [MH⁺] calcd for C₂₇H₁₈ClN₂O₄: 469.0961. Found 469.0950 (0.187 g, 88%).

4.3.7. 4-Chloro-2-(5-((1-(4-fluorophenyl)-5-oxo-3-phenyl-1,5-dihydro-4H-pyrazol-4-ylidene)methyl)furan-2-yl)benzoic acid (3g)

¹H NMR (400 MHz, DMSO-*d*₆): δ 13.44 (s, COOH), 8.768 (d, *J* = 4.0, 1H), 8.010–7.961 (m, 3H), 7.751–7.708 (m, 3H), 7.620–7.581 (m, 4H), 7.531 (s, 1H), 7.335–7.291 (m, 3H). ¹³C NMR (100 MHz, DMSO-*d*₆): 169.0 (C), 162.0 (C), 160.9 (C), 158.5 (C), 157.5 (C), 152.0 (C), 151.0 (C), 136.1 (C), 135.1 (C), 131.5 (CH), 131.3 (CH), 131.1 (C), 130.7 (C), 130.4 (CH), 130.1 (CH), 129.6 (CH), 129.1 (CH), 129.0 (C), 128.7 (CH), 127.8 (C), 121.3 (CH), 121.2 (CH), 120.5 (C), 116.2 (CH), 116.0 (CH), 115.2 (CH). HRMS (*m/z*): [MH[–]] calcd for C₂₇H₁₅ClFN₂O₄: 485.0704. Found 485.0691 (0.297 g, 76%).

4.3.8. 4-Chloro-2-(5-((1-(4-isopropylphenyl)-3-methyl-5-oxo-1,5-dihydro-4H-pyrazol-4-ylidene)methyl)furan-2-yl)benzoic acid (3h)

¹H NMR (400 MHz, DMSO-*d*₆): δ 8.788 (d, *J* = 3.9 Hz, 1H), 7.989 (d, *J* = 2.4 Hz, 1H), 7.892 (d, *J* = 8.8 Hz, 2H), 7.757–7.713 (m, 3H), 7.628–7.587 (m, 4H), 7.535 (s, 1H), 7.361–7.326 (m, 3H), 2.957–2.889 (sep, *J* = 17.1 Hz, 10.1 Hz, 3.3 Hz, 1H), 1.235 (d, *J* = 6.9 Hz, 6H), 1.137 (d, *J* = 6.9 Hz, 6H). ¹³C NMR (100 MHz, DMSO-*d*₆): 169.0 (C), 162.0 (C), 157.4 (C), 151.7 (C), 151.0 (C), 145.8 (C), 136.4 (C), 136.1 (C), 131.5 (C), 131.1 (C), 130.8 (C), 130.3 (C), 130.1 (C), 129.6 (C), 129.2 (C), 129.0 (C), 128.7 (C), 127.6 (C), 127.2 (C), 120.1 (C), 119.5 (C),

115.1 (C), 33.45 (CH–CH₃), 24.35 (CH–CH₃). HRMS (*m/z*): [MH[–]] calcd for C₃₀H₂₂ClN₂O₄: 509.1268. Found 509.1242 (0.095 g, 47%).

4.3.9. (Z)-2-(5-((1-(4-(tert-Butyl)phenyl)-5-oxo-3-phenyl-1,5-dihydro-4H-pyrazol-4-ylidene)methyl)furan-2-yl)-4-chlorobenzoic acid (3i)

¹H NMR (400 MHz, DMSO-*d*₆): δ 8.794 (d, *J* = 3.8 Hz, 1H), 7.981 (d, *J* = 1.6 Hz, 1H), 7.902 (d, *J* = 8.8 Hz, 1H), 7.757–7.719 (m, 3H), 7.629–7.591 (m, 4H), 7.532 (s, 1H), 7.505 (d, *J* = 8.8 Hz, 1H), 7.334 (d, *J* = 3.6 Hz, 1H), 1.311 (s, 1H). ¹³C NMR (100 MHz, DMSO-*d*₆): 169.0 (C), 162.0 (C), 157.4 (C), 151.7 (C), 151.0 (C), 148.0 (C), 136.1 (C), 131.5 (CH), 131.1 (C), 131.0 (CH), 130.8 (C), 130.3 (CH), 130.1 (CH), 129.6 (CH), 129.2 (C), 129.0 (CH), 128.7 (CH), 127.6 (CH), 126.1 (C), 120.7 (C), 119.2 (CH), 115.15 (CH). HRMS (*m/z*): [MH[–]] calcd for C₃₁H₂₄ClN₂O₄: 523.1430. Found 523.1421 (0.065 g, 31%).

4.3.10. 2,5-Diphenyl-4-((5-phenylfuran-2-yl)methylene)-2,4-dihydro-3H-pyrazol-3-one (3j)

¹H NMR (400 MHz, DMSO-*d*₆): 8.811 (d, *J* = 3.2 Hz, 1H), 8.034 (dd, *J* = 1.0 Hz, 8.4 Hz, 2H), 7.960 (d, *J* = 5.2 Hz, 2H), 7.766–7.747 (m, 2H), 7.631 (s, 1H), 7.617–7.585 (m, 3H), 7.521–7.441 (m, 6H), 7.243 (t, *J* = 7.2 Hz, 1H). ¹³C NMR (100 MHz, DMSO-*d*₆): 162.5 (C), 160.4 (C), 151.9 (C), 150.7 (C), 138.6 (C), 131.1 (C), 130.8 (CH), 129.8 (CH), 129.6 (CH), 129.0 (CH), 129.0, 128.8 (CH), 128.7 (CH), 128.4 (CH), 125.2 (CH), 125.0 (CH), 120.2 (C), 119.3 (CH), 110.8 (CH). HRMS (*m/z*): [MH[–]] calcd for C₂₆H₁₉N₂O₂: 391.1447. Found 391.1442 (0.157 g, 69%).

4.3.11. 3-(5-Oxo-3-phenyl-4-((5-phenylfuran-2-yl)methylene)-4,5-dihydro-1H-pyrazol-1-yl)benzoic acid (3k)

¹H NMR (400 MHz, DMSO-*d*₆): δ 13.14 (s, COOH), 8.783 (d, *J* = 1.4 Hz, 1H), 8.623 (t, *J* = 1.8 Hz, 1H), 8.272 (m, 1H), 7.965 (m, 2H), 7.802 (m, 3H), 7.620 (m, 5H), 7.505 (m, 4H). ¹³C NMR (100 MHz, DMSO-*d*₆): 167.5 (C), 162.4 (C), 160.8 (C), 152.5 (C), 150.5 (C), 139.0 (C), 132.1 (C), 131.5 (CH), 130.9 (C), 130.7 (CH), 130.4 (CH), 129.7 (CH), 129.6 (CH), 129.3 (CH), 129.1 (CH), 128.8 (CH), 125.9 (CH), 125.8 (CH), 122.9 (CH), 119.4 (CH), 119.2 (C), 112.2 (CH). HRMS (*m/z*): [MH[–]] calcd for C₂₇H₁₇N₂O₄: 433.1188. Found 433.1183 (0.069 g, 55%).

4.3.12. 3-(3-Methyl-5-oxo-4-((5-phenylfuran-2-yl)methylene)-4,5-dihydro-1H-pyrazol-1-yl)benzoic acid (3l): (e/z mixture)

¹H NMR (500 MHz, DMSO-*d*₆): δ 8.699 (d, *J* = 3.4 Hz, 1H), 8.559 (s, 1H), 8.209 (d, *J* = 7.0 Hz, 1H), 7.978 (d, *J* = 7.5 Hz, 2H), 7.925 (d, *J* = 7.5 Hz, 1H), 7.813 (d, *J* = 4.0 Hz, 1H), 7.760–7.743 (m, 3H), 7.582–7.531 (m, 5H), 7.503–7.450 (m, 3H), 2.749 (s, [3/2] H), 2.358 (s, 3H). ¹³C NMR (125 MHz, DMSO-*d*₆): 162.3 (C), 161.5 (C), 160.1 (C), 151.7 (C), 150.5 (C), 150.0 (C), 148.7 (C), 139.0 (C), 132.0 (C), 131.6 (CH), 130.6 (CH), 130.5 (CH), 130.2 (CH), 129.9 (CH), 129.7 (C), 129.8 (C), 129.0 (C), 128.3 (CH), 127.1 (CH), 125.7 (CH), 125.6 (CH), 125.5 (CH), 122.3 (CH), 122.1 (CH), 121.0 (C), 119.4 (C), 119.0 (CH), 118.7 (CH), 111.9 (CH), 111.7 (CH), 18.32 (CH₃), 13.33 (CH₃). HRMS (*m/z*): [MH[–]] calcd for C₂₂H₁₅N₂O₄: 371.1032. Found 371.1028 (0.057 g, 53%).

4.3.13. 2-(5-((5-Oxo-1,3-diphenyl-1,5-dihydro-4H-pyrazol-4-ylidene)methyl)furan-2-yl)benzoic acid (3m)

¹H NMR (400 MHz, DMSO-*d*₆): δ 13.29 (s, COOH), 8.833 (d, *J* = 4.9 Hz, 1H), 8.024 (dd, *J* = 8.7 Hz, 1.1 Hz, 2H), 7.890 (dd, *J* = 7.7 Hz, 0.7 Hz, 1H), 7.775 (m, 2H), 7.725 (dd, *J* = 7.6 Hz, 1.2 Hz, 1H), 7.653 (m, 5H), 7.527 (m, 3H), 7.266 (m, 2H). ¹³C NMR (100 MHz, DMSO-*d*₆): 169.8 (C), 162.3 (C), 159.6 (C), 152.0 (C), 150.8 (C), 138.7 (C), 132.6 (C), 131.5 (CH), 131.2 (CH), 130.9 (C), 130.5 (CH), 130.4 (CH), 129.6 (CH), 129.4 (CH), 129.3 (CH), 129.0

(CH), 128.6 (C), 128.1 (CH), 127.2 (C), 125.5 (C), 120.0 (C), 119.2 (C), 114.3 (C). HRMS (m/z): $[MH^-]$ calcd for $C_{27}H_{17}N_2O_4$: 433.1188. Found 433.174 (0.223 g, 50%).

4.3.14. 2-(5-((1-(4-Fluorophenyl)-5-oxo-3-phenyl-1,5-dihydro-4H-pyrazol-4-ylidene)methyl)furan-2-yl)benzoic acid (3n)

1H NMR (500 MHz, DMSO- d_6): 8.807 (d, $J = 3.5$ Hz, 1H), 8.021–7.993 (m, 2H), 7.866 (d, $J = 7.5$ Hz, 1H), 7.750–7.704 (m, 3H), 7.651–7.547 (m, 5H), 7.509 (s, 1H), 7.332 (t, $J = 9.0$ Hz, 2H), 7.245 (d, $J = 3.5$ Hz, 1H). ^{13}C NMR (125 MHz, DMSO- d_6): 169.9 (C), 162.1 (C), 160.6 (C), 159.6 (C), 152.0 (C), 150.8 (C), 135.1 (C), 132.6 (C), 131.4 (CH), 131.3 (CH), 130.8 (C), 130.4 (CH), 129.6 (CH), 129.5 (CH), 129.3 (C), 129.0 (CH), 128.6 (C), 128.2 (CH), 127.2 (C), 121.3 (CH), 121.2 (CH), 119.8, 116.2 (CH), 116.0 (CH), 114.3 (CH). HRMS (m/z): $[MH^-]$ calcd for $C_{27}H_{16}FN_2O_4$: 451.1094. Found 451.1095.

4.3.15. (Z)-2-(5-((1-(4-(tert-Butyl)phenyl)-5-oxo-3-phenyl-1,5-dihydro-4H-pyrazol-4-ylidene)methyl)furan-2-yl)benzoic acid (3p)

1H NMR (400 MHz, DMSO- d_6): δ 8.834 (d, $J = 3.9$ Hz, 1H), 7.913 (t, $J = 8.8$ Hz, 3H), 7.764–7.704 (m, 3H), 7.672–7.495 (m, 9H), 7.263 (d, $J = 4.0$ Hz, 1H), 1.312 (s, 9H). ^{13}C NMR (100 MHz, DMSO- d_6): 169.8 (C), 162.1 (C), 159.5 (C), 151.7 (C), 150.8 (C), 148.0 (C), 136.2 (C), 132.6 (C), 131.5 (CH), 131.1 (CH), 130.9 (C), 130.4 (CH), 130.3 (CH), 129.6 (CH), 129.5 (CH), 129.3 (CH), 129.0 (CH), 128.0 (CH), 127.3 (C), 126.1 (CH), 120.1 (C), 119.2 (CH), 114.3 (CH). HRMS (m/z): $[MH^+]$ calcd for $C_{31}H_{26}N_2O_4$: 491.1965. Found 491.1969 (0.080 g, 44%).

4.3.16. 2-(5-((1-(4-Cyanophenyl)-5-oxo-3-phenyl-1,5-dihydro-4H-pyrazol-4-ylidene)methyl)furan-2-yl)benzoic acid (3q)

1H NMR (400 MHz, DMSO- d_6): δ 13.27 (s, COOH), 8.784 (d, $J = 3.9$ Hz, 1H), 8.249 (d, $J = 8.8$ Hz, 2H), 7.947 (d, $J = 8.8$ Hz, 2H), 7.882 (d, $J = 7.4$ Hz, 1H), 7.771 (m, 2H), 7.722 (d, $J = 7.2$ Hz, 1H), 7.604 (m, 5H), 7.538 (s, 1H), 7.271 (d, $J = 3.9$ Hz, 1H). ^{13}C NMR (100 MHz, DMSO- d_6): 169.8 (C), 162.8 (C), 160.1 (C), 153.3 (C), 150.7 (C), 142.1 (C), 134.0 (C), 132.6 (C), 131.8 (C), 131.5 (C), 130.7 (C), 130.5 (C), 129.6 (C), 129.4 (C), 129.1 (C), 128.8 (C), 127.2 (C), 119.3 (C), 118.7 (C), 114.6 (C), 107.0 (C). HRMS(m/z): $[MH^-]$ calcd for $C_{28}H_{16}N_3O_4$: 458.1146. Found 458.1137 (0.121 g, 66%).

4.3.17. 2-(5-((1-(4-Methoxyphenyl)-5-oxo-3-phenyl-1,5-dihydro-4H-pyrazol-4-ylidene)methyl)furan-2-yl)benzoic acid (3r)

1H NMR (400 MHz, DMSO- d_6): δ 13.26 (s, COOH), 8.832 (d, $J = 3.9$ Hz, 1H), 7.884 (m, 3H), 7.758 (m, 3H), 7.650 (m, 5H), 7.509 (s, 1H), 7.252 (d, $J = 4.0$ Hz, 1H), 7.065 (m, 2H), 3.795 (s, 3H). ^{13}C NMR (100 MHz, DMSO- d_6): 169.8 (C), 161.8 (C), 159.4 (C), 157.1 (C), 150.8 (C), 132.6 (C), 131.9 (C), 131.4 (C), 131.0 (C), 130.4 (C), 130.3 (C), 129.6 (C), 129.5 (C), 129.3 (C), 129.0 (C), 127.9 (C), 127.3 (C), 121.3 (C), 120.1 (C), 114.5 (C), 114.2 (C), 55.78 (OCH₃). HRMS(m/z): $[MH^-]$ calcd for $C_{28}H_{20}N_2O_5$: 463.1299. Found 463.1284 (0.157 g, 85%).

4.3.18. 3-(4-(Furan-2-ylmethylene)-5-oxo-3-phenyl-4,5-dihydro-1H-pyrazol-1-yl)benzoic acid (3s)

1H NMR (500 MHz, DMSO- d_6): δ 13.09 (s, COOH), 8.735 (d, $J = 4.0$ Hz, 1H), 8.625 (t, $J = 2.0$ Hz, 1H), 8.289 (s, 1H), 8.260 (dd, $J = 8.0$ Hz, 1.0 Hz, 1H), 7.817 (d, $J = 7.5$ Hz, 1H), 7.779–7.761 (m, 2H), 7.625–7.592 (m, 5H), 6.981 (d, $J = 3.5$ Hz, 1H). ^{13}C NMR (125 MHz, DMSO- d_6): 172.5 (C), 167.5 (C), 162.4 (C), 152.5 (C), 151.7 (CH), 150.7 (C), 138.3 (C), 132.6 (CH), 132.1 (C), 130.6 (C), 130.5 (CH), 129.9 (CH), 129.6 (CH), 129.1 (CH), 126.4 (CH), 126.1 (CH), 123.0 (CH), 120.0 (C), 119.5 (CH), 115.9 (CH). HRMS (m/z):

$[MH^+]$ calcd for $C_{21}H_{15}N_2O_4$: 359.1037. Found 359.1026 (0.094 g, 79%).

4.3.19. (Z)-3-(4-([1,1'-Biphenyl]-4-ylmethylene)-5-oxo-3-phenyl-4,5-dihydro-1H-pyrazol-1-yl)benzoic acid (3t)

1H NMR (400 MHz, DMSO- d_6): δ 13.08 (s, COOH), 8.606 (dd, $J = 2.0$ Hz, 8.4 Hz, 3H), 8.205 (dd, $J = 2.4$, 8.4 Hz, 1H), 7.855–7.727 (m, 8H), 7.575–7.543 (m, 4H), 7.492 (dt, $J = 1.6$ Hz, 7.2 Hz, 2H), 7.4147–7.3942 (m, 1H). ^{13}C NMR (100 MHz, DMSO- d_6): 167.0 (C), 162.3 (C), 162.2 (C), 153.6 (C), 151.4 (C), 149.9 (C), 145.2 (C), 139.2 (C), 138.8 (C), 136.2 (C), 134.5 (C), 132.6 (C), 132.0 (C), 131.3 (C), 130.7 (C), 130.4 (C), 129.7 (C), 128.9 (C), 128.3 (C), 127.9 (C), 126.7 (C), 126.3 (C), 125.4 (C), 122.3 (C), 120.6 (C), 118.8 (C). HRMS (m/z): $[MH^-]$ calcd for $C_{29}H_{19}N_2O_3$: 443.1401. Found 443.1389 (0.163 g, 52%).

4.3.20. (Z)-3-(4-(4-(Benzyloxy)benzylidene)-5-oxo-3-phenyl-4,5-dihydro-1H-pyrazol-1-yl)benzoic acid (3u)

1H NMR (400 MHz, DMSO- d_6): δ 13.14 (s, COOH), 8.630–8.617 (m, 3H), 8.245–8.216 (m, 1H), 7.801–7.740 (m, 1H), 7.731–7.716 (m, 3H), 7.602–7.563 (m, 4H), 7.482–7.461 (m, 2H), 7.423–7.343 (m, 3H), 7.200 (d, $J = 9.2$ Hz, 2H), 5.246 (s, 2H). ^{13}C NMR (100 MHz, DMSO- d_6): 167.5 (C), 163.6 (C), 162.6 (C), 153.8 (C), 151.1 (CH), 138.9 (C), 137.7 (CH), 136.7 (C), 132.0 (C), 130.9 (C), 130.4 (CH), 129.8 (CH), 129.5 (CH), 129.4 (CH), 129.0 (CH), 128.6 (CH), 128.4 (CH), 126.5 (C), 126.0 (CH), 123.1 (CH), 122.7 (C), 119.6 (CH), 115.6 (CH), 70.22 (CH₂). HRMS (m/z): $[MH^-]$ calcd for $C_{30}H_{21}N_2O_4$: 473.1507. Found 473.1501 (0.069 g, 53%).

4.4. Expression and purification of SARS-CoV and MERS-CoV 3CL^{pro}

The expression and purification of SARS-CoV followed our reported procedure.³⁰ For expression of MERS-CoV 3CL^{pro}, the Factor Xa cleavage site (IEGR) and the 3CL^{pro} (accession KJ361502.1, Ser3248–Gln3553) DNA sequence was synthesized and cloned into the pET32 expression vector by Mission Biotech. Company (Taiwan) and was transformed into *Escherichia coli* BL21 (DE3). A 10 ml overnight culture of a single transformant was used to inoculate 1L of fresh LB medium containing 100 μ g/ml ampicillin. The cells were grown at 37 °C to $A_{600} = 0.8$ and induced with 0.4 mM isopropyl- β -thiogalactopyranoside (IPTG) for 22 h at 16 °C. The cells were harvested by centrifugation at 7000 \times g for 15 min and the pellet was suspended in lysis buffer (12 mM Tris-HCl, 120 mM NaCl, 0.1 mM EDTA, and 5 mM DTT, pH 7.5). A French-press instrument (Constant Cell Disruption System) was used to disrupt the cells at 20000 psi and centrifuged at 20,000 \times g for 1 h to discard the debris. The cell-free extract was loaded onto Ni-NTA column which was equilibrated with lysis buffer containing 5 mM imidazole. After exhaustive washing with lysis buffer, the imidazole concentration of the washing buffer was increased to 30 mM. The protein eluted by lysis buffer with 300 mM imidazole were dialyzed against lysis buffer to removed imidazole and then Factor Xa was added to the fusion proteins to a final concentration of 1% (w/w) and incubated at 16 °C for 24 h to remove the His-tag. Subsequently, the processed MERS-CoV 3CL^{pro} was passed through a Ni-NTA column for purification. The protein concentration was determined by the protein assay kit (BioRad, USA) and BSA was used as standard.

4.5. Measurement of IC₅₀

A fluorometric assay³⁰ was utilized to determine the inhibition constants of the prepared samples. Fluorogenic peptide, Dabcyl-KTSAVLQSGFRKME-Edans, was used as the substrate, and the enhanced fluorescence due to the cleavage of this substrate

catalyzed by the 3CL^{pro} was monitored at 538 nm with excitation at 355 nm. The IC₅₀ value of the individual sample was measured in a reaction mixture containing 50 nM SARS 3CL^{pro} or 300 nM MERS-Cov 3CL^{pro} and 10 μM of the fluorogenic substrate in 20 mM Bis-Tris (pH 7.0).

Acknowledgement

This work was supported by Academia Sinica, Taiwan.

Supplementary data

Supplementary data associated with this article can be found, in the online version, at <http://dx.doi.org/10.1016/j.bmc.2016.05.013>.

References and notes

- Rota, P. A.; Oberste, M. S.; Monroe, S. S.; Nix, W. A.; Campagnoli, R.; Icenogle, J. P.; Penaranda, S.; Bankamp, B.; Maher, K.; Chen, M. H.; Tong, S.; Tamin, A.; Lowe, L.; Frace, M.; DeRisi, J. L.; Chen, Q.; Wang, D.; Erdman, D. D.; Peret, T. C.; Burns, C.; Ksiazek, T. G.; Rollin, P. E.; Sanchez, A.; Liffick, S.; Holloway, B.; Limor, J.; McCaustland, K.; Olsen-Rasmussen, M.; Fouchier, R.; Gunther, S.; Osterhaus, A. D.; Drosten, C.; Pallansch, M. A.; Anderson, L. J.; Bellini, W. J. *Science* **2003**, *300*, 1394.
- Thiel, V.; Herold, J.; Schelle, B.; Siddell, S. G. *J. Virol.* **2001**, *75*, 6676.
- Thiel, V.; Ivanov, K. A.; Putics, A.; Hertzog, T.; Schelle, B.; Bayer, S.; Weissbrich, B.; Snijder, E. J.; Rabenau, H.; Doerr, H. W.; Gorbalenya, A. E.; Ziebuhr, J. *J. Gen. Virol.* **2003**, *84*, 2305.
- Kuo, C. J.; Liang, P. H. *ChemBioEng. Rev.* **2015**, *2*, 118.
- Kumar, V.; Jung, Y. S.; Liang, P. H. *Expert Opin. Ther. Pat.* **2008**, *23*, 1337.
- Baez-Santos, Y. M.; St John, S. E.; Mesecar, A. D. *Antivir. Res.* **2015**, *115*, 21.
- Ramajayam, R.; Tan, K. P.; Liang, P. H. *Biochem. Soc. Trans.* **2011**, *39*, 1371.
- Zhao, Q.; Weber, E.; Yang, H. *Recent Pat. Antiinfect. Drug Discov.* **2013**, *8*, 150.
- Tong, T. R. *Expert Opin. Ther. Pat.* **2009**, *19*, 415.
- Hilgenfeld, R.; Peiris, M. *Antivir. Res.* **2013**, *100*, 286.
- WHO, Middle East respiratory syndrome coronavirus (MERS-CoV), <http://www.who.int/mediacentre/factsheets/mers-cov/en/> (10.05.16).
- Tomar, S.; Johnston, M. L.; St John, S. E.; Osswald, H. L.; Nyalapatla, P. R.; Paul, L. N.; Ghosh, A. K.; Denison, M. R.; Mesecar, A. D. *J. Biol. Chem.* **2015**, *290*, 19403.
- Kilianski, A.; Baker, S. C. *Antivir. Res.* **2014**, *101*, 105.
- Barnard, D. L.; Kumaki, Y. *Future Virol.* **2011**, *6*, 615.
- Krug, R. M.; Lamb, R. A. *Orthomyxoviridae: The Viruses and their Replication*, 4th ed.; Lippincott Williams and Wilkins: Philadelphia, 2001.
- Watanabe, Y.; Ibrahim, M. S.; Suzuki, Y.; Ikuta, K. *Trends Microbiol.* **2012**, *20*, 11.
- Taubenberger, J. K.; Morens, D. M. *Emer. Infect. Dis.* **1918**, *12*, 15.
- Gao, R. B.; Cao, B.; Hu, Y. W.; Feng, Z. J.; Wang, D. Y.; Hu, W. F.; Chen, J.; Jie, Z. J.; Qiu, H. B.; Xu, K.; Xu, X. W.; Lu, H. Z.; Zhu, W. F.; Gao, Z. C.; Xiang, N. J.; Shen, Y. Z.; He, Z. B.; Gu, Y.; Zhang, Z. Y.; Yang, Y.; Zhao, X.; Zhou, L.; Li, X. D.; Zou, S. M.; Zhang, Y.; Li, X. Y.; Yang, L.; Guo, J. F.; Dong, J.; Li, Q.; Dong, L. B.; Zhu, Y.; Bai, T.; Wang, S. W.; Hao, P.; Yang, W. Z.; Zhang, Y. P.; Han, J.; Yu, H. J.; Li, D. X.; Gao, G. F.; Wu, G. Z.; Wang, Y.; Yuan, Z. H.; Shu, Y. L. *N. Engl. J. Med.* **2013**, *368*, 1888.
- CDC. Avian Influenza A (H7N9) Virus. <http://www.cdc.gov/flu/avianflu/h7n9-virus.htm> (accessed 10.05.16).
- Kumar, V.; Chang, C. K.; Tan, K. P.; Jung, Y. S.; Chen, S. H.; Cheng, Y. S.; Liang, P. H. *Org. Lett.* **2014**, *16*, 5060.
- Ramajayam, R.; Tan, K. P.; Liu, H. G.; Liang, P. H. *Bioorg. Med. Chem.* **2010**, *18*, 7849.
- Racane, L.; Tralic-Kulenovic, V.; Boykin, D. W.; Karminski-Zamola, G. *Molecules* **2003**, *8*, 342.
- Fan, K.; Wei, P.; Feng, Q.; Chen, S.; Huang, C.; Ma, L.; Lai, B.; Pei, J.; Liu, Y.; Chen, J.; Lai, L. *J. Biol. Chem.* **2004**, *279*, 1637.
- Hsu, M. F.; Kuo, C. J.; Chang, K. T.; Chang, H. C.; Chou, C. C.; Ko, T. P.; Shr, H. L.; Chang, G. G.; Wang, A. H. J.; Liang, P. H. *J. Biol. Chem.* **2005**, *280*, 31257.
- Hu, T. C.; Zhang, Y.; Li, L. W.; Wang, K. F.; Chen, S.; Chen, J.; Ding, J. P.; Jiang, H. L.; Shen, X. *Virology* **2009**, *388*, 324.
- Sisk, J. M.; Frieman, M. B. *ACS Infect. Dis.* **2015**, *1*, 401.
- de Wilde, A. H.; Jochmans, D.; Posthuma, C. C.; Zevenhoven-Dobbe, J. C.; van Nieuwkoop, S.; Bestebroer, T. M.; van den Hoogen, B. G.; Neyts, J.; Snijder, E. J. *Antimicrob. Agents Chemother.* **2014**, *58*, 4875.
- Dyall, J.; Coleman, C. M.; Hart, B. J.; Venkataraman, T.; Holbrook, M. R.; Kindrachuk, J.; Johnson, R. F.; Olinger, G. G.; Jahrling, P. B.; Laidlaw, M.; Johansen, L. M.; Lear-Rooney, C. M.; Glass, P. J.; Hensley, L. E.; Frieman, M. B. *Antimicrob. Agents Chemother.* **2014**, *58*, 4885.
- Kuo, C. J.; Liu, H. G.; Lo, Y. K.; Seong, C. M.; Lee, K. I.; Jung, Y. S.; Liang, P. H. *FEBS Lett.* **2009**, *583*, 549.
- Kuo, C. J.; Chi, Y. H.; Hsu, J. T.; Liang, P. H. *Biochem. Biophys. Res. Commun.* **2004**, *318*, 862.